IOP Conference Series: Materials Science and Engineering

PAPER • OPEN ACCESS

Synthesis and electric transportation properties of high-entropy oxides based on cerium oxide

To cite this article: M N Yapryntsev *et al* 2021 *IOP Conf. Ser.: Mater. Sci. Eng.* **1014** 012059

Synthesis and electric transportation properties of high-entropy oxides based on cerium oxide

M N Yapryntsev[1*], I V Sudzhanskaya[1], R A Lyubushkin[2], E N Yapryntseva[1]

[1]Belgorod State University, Belgorod, 308015, Russian Federation
[2]Belgorod State Technological University Named After V.G. Shukhov, Belgorod, 308012, Russian Federation

*Corresponding author: yaprintsev@bsu.edu.ru

Abstract. CeGdRLaPr$O_{2-\delta}$ (where R: La, Y and Dy) rare-earth high-entropy oxides (HEOx) with the Ia-3 (206) structure were obtained. The structural, microstructural and transport properties of the compounds were studied. All samples exhibiting good homogeneity and electrical conductivity typical of materials for the manufacture of solid electrolytes.

1. Introduction

The idea of developing high-entropy oxides was borrowed from the accumulated research experience in the design of high-entropy alloys [1]. In the literature, the first works in this area have been found since 2015. For the first time, an entropy-stabilized (CoCuMgNiZn)O solid solution with the structure Fm-3m was synthesized [2]. Since then, a number of studies have been published on both the properties of these oxides [3] and the search for new high-entropy oxide systems. As a result, the range of known high-entropy oxides has expanded significantly. Despite a very early stage of their development, oxides with high entropy have already shown great promise as functional materials, demonstrating, for example, colossal dielectric constant, high ionic conductivity [4] and low thermal conductivity. Some of the high-entropy oxides have been successfully tested as anode materials for lithium-ion batteries or cathode materials for Na-ion cells [1-4].

In this work, single-phase high-entropy oxides of the composition (CeGdDySmPr)$O_{2-\delta}$, (CeGdYSmPr)$O_{2-\delta}$ and CeGdLaSmPr$O_{2-\delta}$ were obtained for the first time. These materials were synthesized by the sol-gel method followed by cold uniaxial compaction and free sintering at 1500 °C in air. Comprehensive studies of structural, microstructural and electrical transport properties were carried out. The results of studying the electrical transport properties demonstrate a similarity with the properties of classical systems based on cerium oxides ($Ce_{0.8}Pr_{0.2}O_{2-\delta}$).

2. Materials and methods

Cerium(III) nitrate hexahydrate ($Ce(NO_3)_3 \cdot 6H_2O$, 99.9%), gadolinium (III) acetate tetrahydrate ($Gd(CH_3COO)_3 \cdot {}_4H_2O$, 99.9%), dysprosium (III) acetate tetrahydrate ($Dy(CH_3COO)_3 \cdot 4H_2O$, 99.9%), samarium (III) nitrate hexahydrate ($Sm(NO_3)_3 \cdot 6H_2O$, 99.9%), praseodymium (III) acetate sesquihydrate ($Pr(NO_3)_3 \cdot 6H_2O$, 99.9%), lanthanum (III) nitrate hexahydrate ($La(NO_3)_3 \cdot 6H_2O$, 99.9%), ytrium (III) acetate tetrahydrate ($Y(CH_3COO)_3 \cdot 4H_2O$, 99.9%), 28−30% ammonium hydroxide (NH_4OH) and deionized water were used for the synthesis. Starting materials were weighted in a way to maintain equimolar proportions of the cations and then they were dissolved in 100 ml of deionized water. The pH

of the solution was adjusted by adding 28% NH_4OH dropwise until the pH reached ~11. The solution was stirred for 1 h, then the resulting gel was evaporated at a temperature of 120 °C until complete drying. In the second step, the obtained precursors were annealed at a temperature of 900 ˚C for 2 hours in an air atmosphere. Next, all samples were pressed into pellets of 20 mm diameter, under pressure of 200 MPa, using a uniaxial hydraulic press. The pellets were then free-sintered in a chamber furnace for 4 h at 1500 °C, and subsequently cooled down to room temperature with the furnace.

The morphology and size of the powder particles were identified by transmission electron microscopy (TEM Jeol 2100). The crystal structure was examined by x-ray diffraction (UltimaIV). The element composition and microstructure of specimens was controlled by scanning electron microscopy Quanta 200 3D with EDS (energy dispersive spectroscopy) detector. The specific electrical conductivity (σ) of the AC was measured on a Novocontrol Concept 43 impedance meter using a four-probe method.

3. Results and discussion

Figure 1 (a) presents the XRD diffractograms of the studied HEO ($CeGdDyLaPrO_{2-\delta}$, $CeGdDyLaPrO_{2-\delta}$ and $CeGdDyLaPrO_{2-\delta}$) samples after annealing at a temperature of 900 °C. Already at this stage of obtaining powdery materials, all the samples under study are single-phase, (body-centered cubic) and the peaks corresponding to space symmetry group Ia-3 (206).

The changes in the lattice parameters for the samples are reflected in the corresponding changes in the position of the diffraction peaks, as shown, for example, for the peak (2 2 2) (Figure 1 (a)).. The lattice parameters calculated by the Rietveld refinement for all the samples are presented in Figure 1 (b). The parameters increase with increasing ionic radius ($r_{ion}(R^{+3})$) of the variable element. Significant structural changes of all materials during sintering were not observed, the values of the lattice parameters were constant.

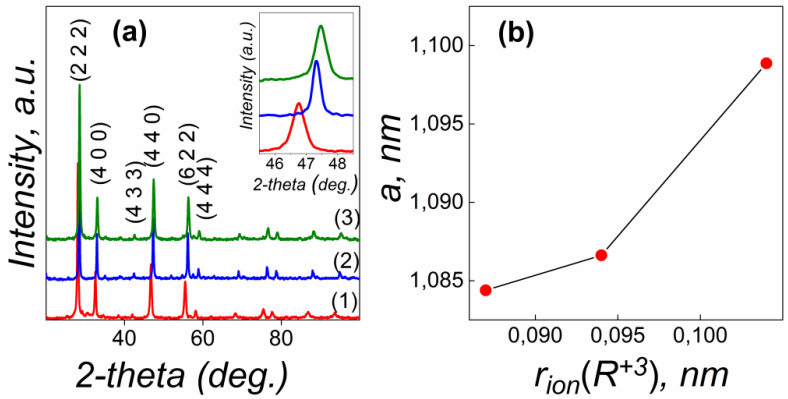

Figure 1. The XRD patterns (a) of $CeGdLaSmPrO_{2-\delta}$ (1), $CeGdDySmPrO_{2-\delta}$ (2), and $CeGdYSmPrO_{2-\delta}$ (3) and ionic radius of the variable element effect on the lattice parameters (b)

Typical morphology of powders annealed at 900 ˚C are presented at Figure 2. The results of TEM investigation of the synthesized powders demonstrate a similar pattern for all compositions. The typical morphology of $CeGdLaSmPrO_{2-\delta}$ powders are presented in Figure 2. After heat treatment, the nanoparticles of $CeGdLaSmPrO_{2-\delta}$ have an irregular shape. To estimate the average size of nanoparticles in the powder of $CeGdLaSmPrO_{2-\delta}$, histograms of the particles size distribution were plotted using the TEM images in Figure 2 (b). Next, these histograms were analyzed by lognormal unimodal distribution fittings. It is shown that the nanoparticles have an average size of 28 nm, with a standard deviation of ±7 nm.

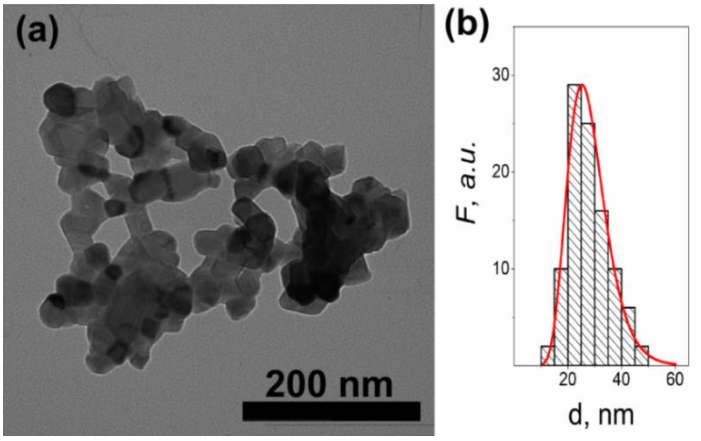

Figure 2. Typical TEM image for example of $CeGdLaSmPrO_{2-\delta}$ starting powders (a) and histogram of the nanoparticles size distribution (b)

The elemental analysis of $CeGdRLaPrO_{2-\delta}$ (where R: La, Y and Dy) was measured by scanning electron microscopy-energy dispersive spectroscopy (SEM-EDS). EDS - analysis shows that the element composition ofthe tested powders corresponded to the nominal composition. This reveals that the nanoparticles are composed of the stoichiometric phase of $CeGdRLaPrO_{2-\delta}$ (where R: La, Y and Dy).

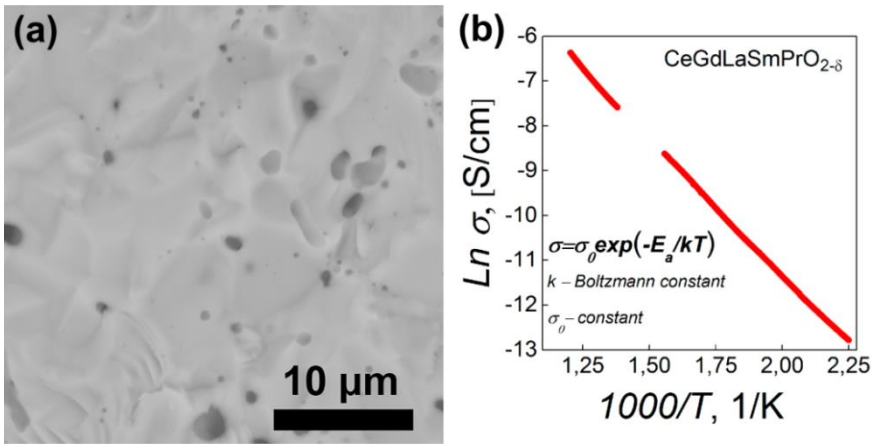

Figure 3. Typical microsctructure of the fracture surface of bulk samples for example of $CeGdLaSmPrO_{2-\delta}$ (a) and temperature dependence of the electrical conductivity in lnσ (1/T) coordinates (b)

A SEM image of the fractured surface sow of the exemplary samples are presented in Figure 3 (a). The SEM image obtained in a phase contrast mode (detector-BSD) show that the bulk samples are phase homogeneous and have a disordered grain structure with an average size of grains ~ 3,3 µm. Closed pores are observed on the fractured surface. As can be seen from the presented EDS data, the obtained samples are close to the assumed equimolar composition, with the only exception related to the lower content of Pr (Table 1). The presence of pores and the violation of stoichiometry most probably resulted from the evaporation of Pr during thermal treatment, as indicated by the bluish residues visible in the alumina crucibles. According to the results of the EDS analysis, all samples on average, the concentration of praseodymium decreases about 1.5 at.% relative to the pre assigned stoichiometric composition.

Electrical conductivity (σ) was measured in the temperature range from room temperature to 800 °C in air. Figure 3 (b) shows the temperature dependence of the electrical conductivity of the

$CeGdLaSmPrO_{2-\delta}$ ceramic system in $\ln\sigma(1/T)$ coordinates according to the Arrhenius law (see the corresponding equation in figure 3 (b)). [5]

Table 1. Average composition of the studied materials derived from EDS area analysis of bulk samples

Sample	Element (At. %)							
	Ce	Gd	La	Dy	Y	Sm	Pr	O
$CeGdLaSmPrO_{2-\delta}$	8.0	7.9	7.7	-	-	7.8	6.0	62.6
$CeGdDySmPrO_{2-\delta}$	8.3	7.7	-	7.8	-	7.4	5.9	62.9
$CeGdYSmPrO_{2-\delta}$	7.9	7.8	-	-	7.6	7.7	6.1	62.9

The values of the activation energy (E_a) of the conduction process, calculated for two temperature (T) range, from 170 to 400 °C and from 460 to 560 °C. It was found that both in the low-temperature region (170 °C - 400 °C) and in the middle-temperature region (450 ° - 560 °), the activation energy of the $CeGdLaSmPrO_{2-\delta}$ ceramic system remained practically unchanged, amounting to 0.52 eV and 0.53 eV, which is associated with a constant mechanism of oxygen-ionic conductivity caused by the drift motion of oxygen ions under the influence of an external electric field in a given temperature range [6-8]. The electrical conductivity of the obtained ceramics at a temperature of 510 °C reaches $0.1 \cdot 10^{-2}$ S/cm, which meets the requirements for the ionic conductivity of materials for the manufacture of solid electrolytes [6], and corresponds to materials based on cerium oxide.

4. Conclusion

In this work, three different compositions from the $CeGdRLaPrO_{2-\delta}$ (where R: La, Y and Dy) systems were prepared using the method of sol-gel synthesis and sintering at 1500 °C. All the samples under study are single-phase, (body-centered cubic), and the peaks correspond to that space symmetry group Ia-3 (206). Based on the evolution of the lattice constants, as well as the EDS-spectroscopy data, it can be stated that the received materials are composed of the stoichiometric phase of $CeGdRLaPrO_{2-\delta}$ (where R: La, Y and Dy). The synthesized initial powders are nanosized, with an average particle size of 28 nm. When nanopowders are sintered, bulk materials are obtained. Sintering at 1500 °C leads to partial evaporation of praseodymium, which is confirmed by the EDS method. In the low-temperature region (170 °C - 400 °C) and in the middle-temperature region (450 °C - 560 °C), the activation energy of electrical conductivity of the $CeGdLaSmPrO_{2-\delta}$ ceramic system remained practically unchanged, amounting to 0.52 eV and 0.53 eV. The electrical conductivity of the obtained ceramics at a temperature of 510 °C reaches $0.1 \cdot 10^{-2}$ S/cm, which meets the requirements for the ionic conductivity of materials for the manufacture of solid electrolytes.

References

[1] Cantor B, Chang I T, Knight P and Vincent A J, 2004 *Sci. Eng: A* **375-377** 213–218.
[2] Rost C M, Schaet R, Borman T, Moballegh A, Dickey E C, Hou D, Jones J L, Curtarolo S and Maria J P, 2015 *Nat. Commun.* **6** 8485.
[3] Rost C M, Rak Z, Brenner D W and Mari J P, 2017 *J. Am. Ceram. Soc.* **100** 2732–2738.
[4] Bérardan D, Franger S, Meena A K and Dragoe D, 2016 *J. Mater. Chem. A.* **4** 9536–9541.
[5] Panigrahi S, Biswa R C, Anwar S, Besra L and Bhattacharjee S, 2013 *J. Am. Ceram. Soc.* **96** 2846–2851.
[6] Skinner S J and Kilner J A, 2003 *Materials Today* **6** 30-37
[7] Dąbrowa J, Szymczak M, Zajusz M, Mikuła A, Moździerz M, Berent K, Wytrwal-Sarna M, Bernasik A, Stygar M and Świerczek K, 2020 *Journal of the European Ceramic Society* **40** 5870-5881.
[8] Yahiro H, Eguchi Y, Eguchi K and Arai H, 1988 *J.of Applied Electrochemistry* **18** 527-531.